A theoretical study of vacuum force on gravity foils and step foils

JEAN W. ZU AND JIANBIN CHEN

ABSTRACT

During sheet formation on a fourdrinier table, the rate of water removal is predominantly controlled by the vacuum forces generated by drainage devices. This work proposes equations for calculating the vacuum forces on gravity foils and step foils. The proposed equations—based on the theory of lubrication—are then validated by testing experimental data from the literature. The results indicate that the equations can simulate peak vacuum forces and vacuum profiles on both types of foils.

Application:

Equations for calculating vacuum forces generated by the gravity foils and step foils that are used to enhance drainage on fourdrinier tables.

GRAVITY FOILS AND STEP FOILS are the most common types of foils used on modern fourdrinier tables. Several experimental studies of the vacuum forces generated by these foils have been published. However, there is very limited information available on theoretical equations to calculate these vacuum forces. This study proposes a theoretical approach based on the theory of lubrication. The equations developed using this approach can be used to calculate vacuum forces on both gravity and step foils.

Schiher and Getman *(1)* have measured vacuum profiles produced by gravity foils and step foils. **Figure 1** shows the vacuum profiles they observed for a step foil and for a 3° gravity foil. The peak vacuum on a gravity foil was measured at about 35 cm H_2O, while that on a step blade was about 120 cm H_2O. Both vacuum measurements are exclusive of box vacuum. Figure 1 also shows that the peak vacuum on the gravity foil is located close to the tail of the foil, while the peak vacuum of the step foil occurs in the front part of the foil, immediately following the step.

A step foil can generate a variety of pressure profiles depending upon its length, the step depth, machine speed, etc. **Figures 2 and 3** illustrate vacuum profiles over step foils at wire speeds of 7.67 m/s (1500 ft/min). These data were collected by Schiher and Getman *(1)* during an investigation of critical step depth. Each figure represents two successive trials (A and B) involving a change in step depth large enough to prevent a vacuum pulse from forming. Trial A represents a typical step foil pulse, while Trial B simulates the pulse of a slotted low-vacuum drainage element.

APPLICATION OF LUBRICATION THEORY TO CALCULATE VACUUM FORCE

Equations to calculate vacuum forces on gravity foils and step foils were developed from lubrication theory. According to lubrication theory *(2)*, if a bearing film is to support a load, the pressure of the film must exceed the ambient pressure, as shown in **Fig. 4** for a slider bearing. For both compressible film (i.e., gas) and incompressible film (i.e., water and oil), the pressure gradient is positive in Region I and negative in Region II.

The behavior of a lubricated slider bearing is remarkably similar to the behavior of a foil on a fourdrinier table. The static foil serves as a slider bearing, while the fabric serves as the moving part. In the papermaking case, however, the slider bearing (the foil) is upside down, while the moving part (the fabric) is on top. **Figure 5** illustrates this configuration for a gravity foil (top) and a step foil (bottom).

In this study, a gravity foil is likened to a tapered flat slider bearing, while a step foil is modeled as a step slider bearing. The only difference is that there is a small gap, h_2, in bearings, while there is no such a gap between the foil and the forming fabric on a fourdrinier table. However, considering that the fabric is moving very fast with downward and upward accelerations, it can be assumed that there is a very tiny gap—a layer of slurry—between the wire and the foil. Using this assumption, it is possible to apply the lubrication equations for tapered flat slider bearings and step slider bearings directly to gravity foils and step foils, respectively.

Step slider bearing—step foil

Rayleigh *(3)* was the first person to study optimum load-bearing shape on a step slider bearing using thick-film lubrication theory. He applied the calculus of variations to determine the optimum geometry for the incompressible film. Rayleigh's analysis was extended by Charnes *et al. (4)* to include pressure-dependent viscosity and, more recently, by Maday *(5)* to verify that the optimum slider contains only one step. The optimum film shape obtained by Rayleigh is defined by the step bearing, as shown in **Fig. 6**, with the bearing length ratio defined as $\lambda = B_2/B_1$.

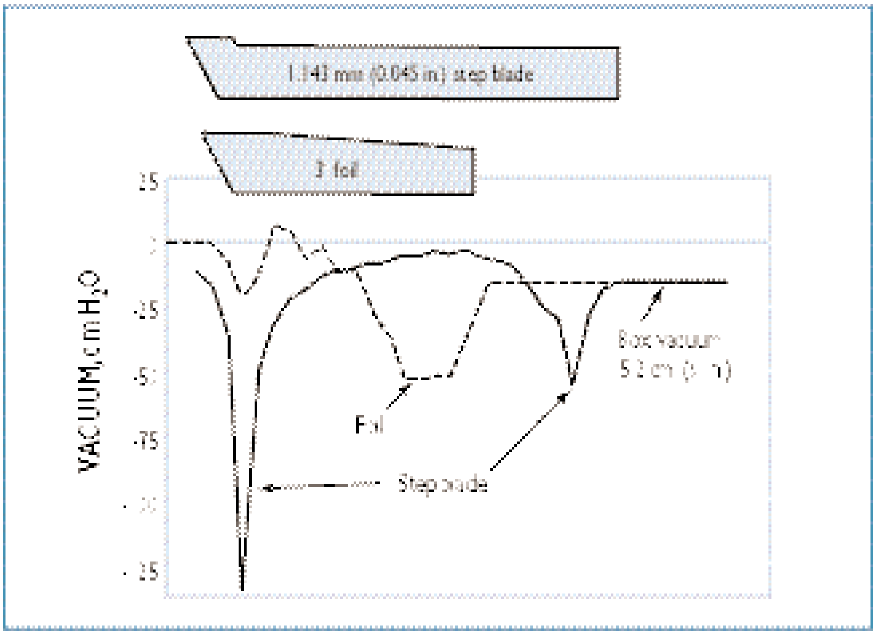

1. Vacuum profiles on a 3° gravity foil and a 1.14-mm step foil (data from Schiher and Getman **(1)***)*

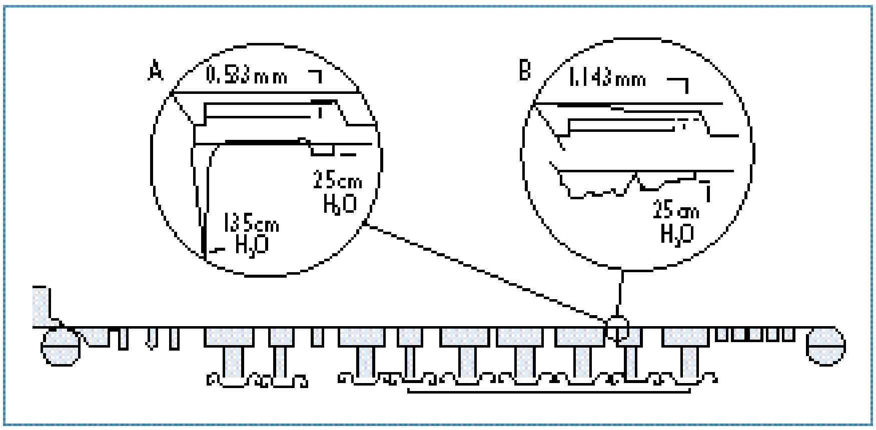

2. Shapes of vacuum pulse at step depths of 0.53 mm and 1.14 mm (data from Schiher and Getman **(1)***); Step Foil I*

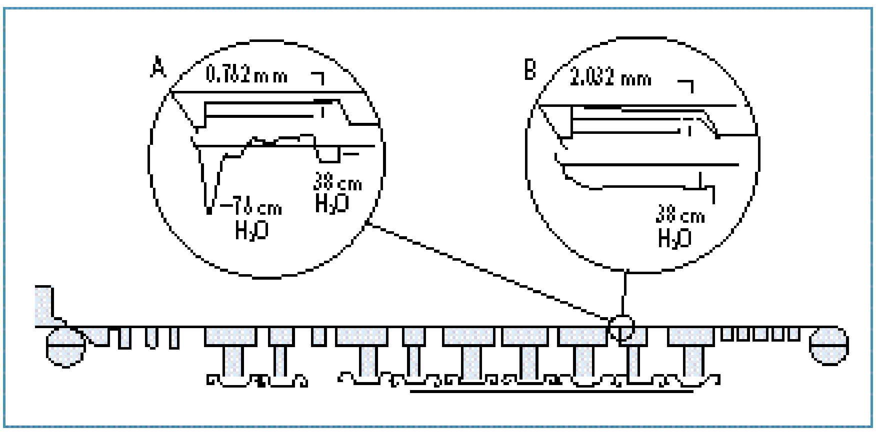

3. Shapes of vacuum pulse at step depths of 0.76 mm and 2.03 mm (data from Schiher and Getman **(1)***); Step Foil II*

By assuming the pressure to be continuous, the load capacity can be easily computed. Since the pressure gradient at each section is constant, the pressure profile must be triangular, with the peak pressure occurring at the film-thickness discontinuity. The peak pressure $P_{step—max}$ is defined in Eq. 1

$$P_{step—max} = \frac{\Lambda\lambda(H_1 - 1)}{(\lambda H_1^3 + 1)(\lambda + 1)} \qquad (1)$$

and local pressure is defined in Eq. 2

$$P_{step} = 1 + P_{step—max}\frac{X}{1 + \lambda}$$

$$\text{when } X \le (1 + \lambda)^{-1} \qquad (2a)$$

$$P_{step} = 1 + P_{step—max}\frac{(1 + \lambda)X - 1}{\lambda}$$

$$\text{when } X > (1 + \lambda)^{-1} \qquad (2b)$$

where

$\Lambda = \dfrac{6\mu V_w B}{h}$

P_a = atmospheric pressure

μ = viscosity

$H_1 = h_1/h_2$

$H = H_1 - (H_1 - 1)X$

$B = B_1 + B_2$

$X = x/B$

$0 \le x \le B$

$\lambda = B_2/B_1$

Equation 1 defines the peak pressure and Eq. 2 defines the pressure distribution on the step bearing. As assumed previously, these equations can be applied directly to step foils. In order to use Eq. 1 to calculate peak pressure on a step foil, it is rewritten as

$$P_{step\ foil—max} = \frac{6\mu V_w B\lambda(H_1 - 1)}{h_2^2 P_a(\lambda H_1^3 + 1)(\lambda + 1)} \qquad (3)$$

while Eq. 2 for the vacuum distribution is rewritten as

$$P_{step\ foil} = 1 + \frac{6\mu V_w B\lambda(H_1 - 1)}{h_2^2 P_a(\lambda H_1^3 + 1)(\lambda + 1)}\ \frac{X}{1 + \lambda}$$

$$\text{when } X \le (1 + \lambda)^{-1} \qquad (4a)$$

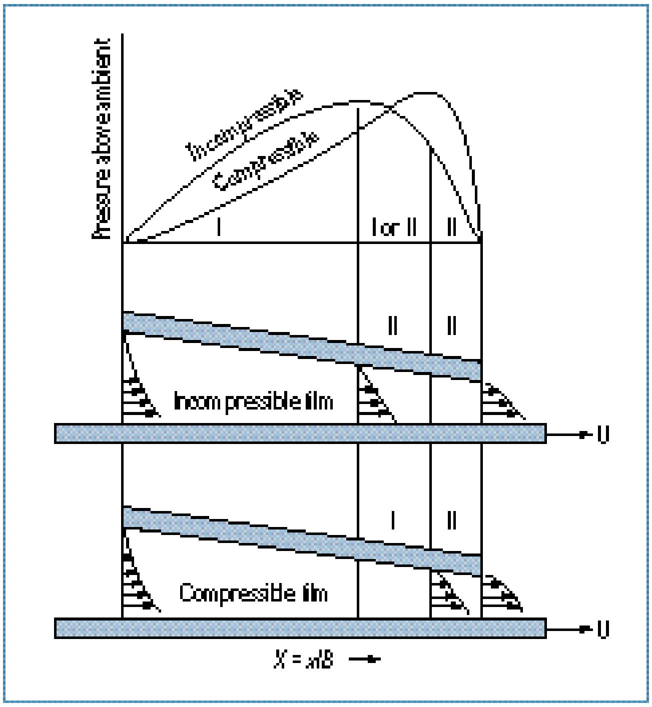

4. Velocity profiles and pressure distribution of compressible and incompressible lubricating films for a slider bearing (from **Fluid Film Lubrication**, *John Wiley & Sons)*

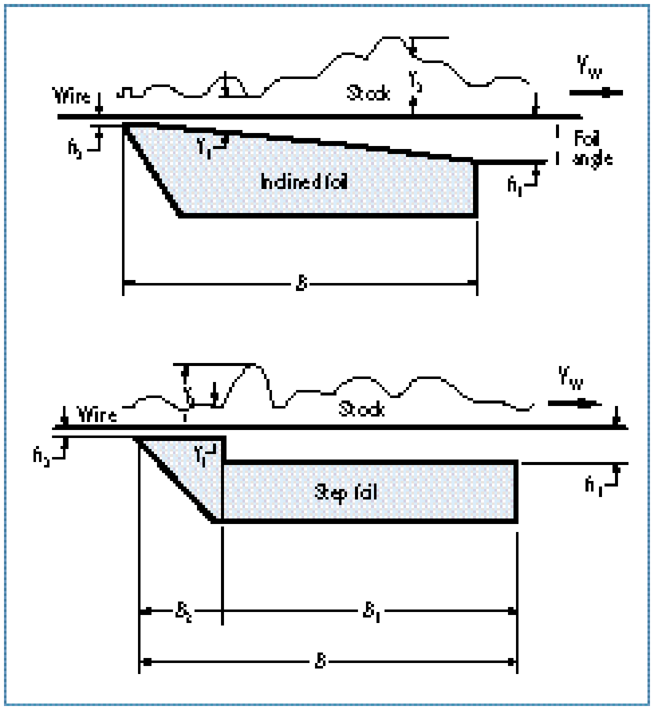

5. Diagrams of a gravity foil (top) and a step foil (bottom)

$$P_{\text{step foil}} = 1 + \frac{6\mu V_w B \lambda (H_1 - 1)}{h_2^2 P_a (\lambda H_1^3 + 1)(\lambda + 1)} \frac{(1+\lambda)X - 1}{\lambda}$$

when $X > (1 + \lambda)^{-1}$ (4b)

Tapered flat slider bearing—gravity foil

A tapered flat slider bearing is illustrated in **Fig. 7**. The pressure in the converging section rises parabolically and peaks just ahead of the junction between the sections. At the junction point, the pressure is greater than the ambient pressure. This high pressure at the leading edge of the parallel section occurs without a film-thickness discontinuity, in contrast to the case with the step bearing.

The analysis of limiting conditions for the tapered flat slider bearing is similar to that of a step bearing. For the limiting incompressible condition, the pressure can be written as

$$P_{\text{gravity}} = 1 + \Lambda \frac{(H_1 - H)[2H_1 H - H^*(H_1 + H)]}{2H_1^2 H^2 (H_1 - 1)(1 - \lambda)}$$

when $X < B_1/B_2$ (5a)

$$P_{\text{gravity}} = 1 + \Lambda \frac{(H_1 - 1)(1 - X)(1 + \lambda)}{(1 + \lambda)(2\lambda H_1^2 + H_1 + 1)}$$

when $X > B_1/B_2$ (5b)

where

$$H^* = \frac{2H_1(1 + \lambda H_1)}{2\lambda H_1^2 + H_1 + 1}$$

Equations 5a and 5b define the pressure distribution on the tapered flat slider bearing. Again, as assumed previously, these equations can be applied directly to gravity foils by rewriting them as

$$P_{\text{gravity foil}} = 1 + \left(\frac{6\mu V_w B}{h_2^2 P_a}\right) \left(\frac{(H_1 - H)[2H_1 H - H^*(H_1 + H)]}{2H_1^2 H^2 (H_1 - 1)(1 - \lambda)}\right)$$

when $X < B_1/B_2$ (6a)

$$P_{\text{gravity foil}} = 1 + \left(\frac{6\mu V_w B}{h_2^2 P_a}\right) \left(\frac{(H_1 - 1)(1 - X)(1 + \lambda)}{(1 + \lambda)(2\lambda H_1^2 + H_1 + 1)}\right)$$

when $X > B_1/B_2$ (6b)

RESULTS AND DISCUSSION

In the previous section, equations were developed to calculate the vacuum forces on step foils (Eq. 4) and on gravity foils (Eq. 6). In this section, these equations are used to calculate vacuum forces based on data published by Schiher and Getman *(1)*.

Vacuum force on gravity foil

The vacuum profile on a 3° gravity foil was calculated from Eq. 6 using the values listed in **Table I**. Values for the variables correspond to the conditions cited by Schiher and Getman *(1)*. By feeding these values into Eq. 6, the vacuum forces at various positions across the foil can be calculated. These results are presented in **Table II** and plotted in **Fig. 8**.

The calculated results in Fig. 8 are similar to the experimental results in Fig. 1. The calculated peak value was about 32 cm H_2O, which is very close to the peak vacuum in Fig. 1, about 35 cm H_2O (exclusive of box vacuum). Moreover, the shape of the calculated vacuum profile in Fig. 8 is similar to that observed in Fig. 1. Finally, the peak vacuum was calculated at X = 0.8, near the tail of the

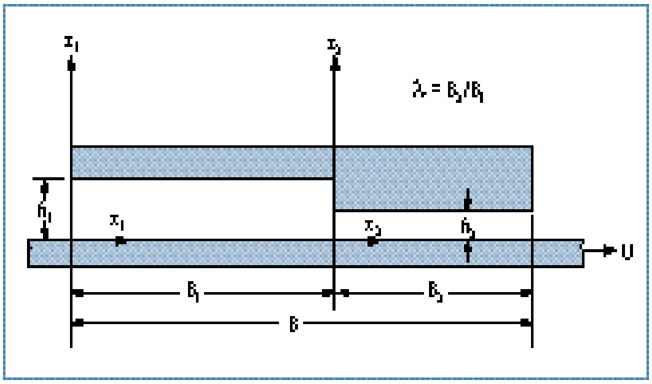

6. Step slider bearing with length ratio $\lambda = B_2 / B_1$ (from **Fluid Film Lubrication**, *John Wiley & Sons)*

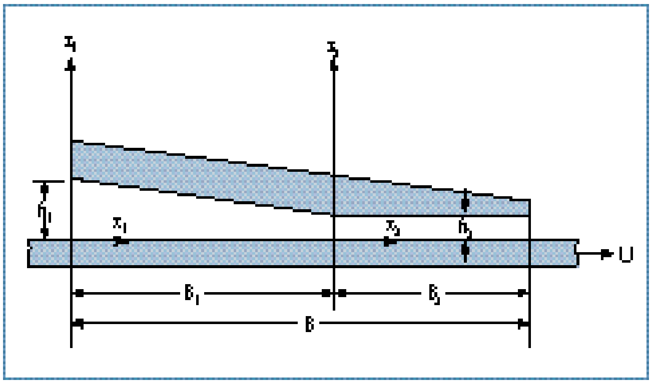

7 Tapered flat slider bearing (from **Fluid Film Lubrication**, *John Wiley & Sons)*

V_w	8.64 m/s (1700 ft/min)
B_1	50.8 mm
B_2	20.0 mm
h_1	3.66 mm
h_2	1.0 mm
X	0–1.0 (intervals of 0.1)
μ	0.001 N·s/m^2
P_a	1.0133 × 10^5 N/m^2

* Values correspond to conditions reported by Schiher and Getman *(1)*.

*I. List of variables required to calculate vacuum forces on a 3° gravity foil using Eq. 6**

X	Calculated vacuum force, cm H_2O
0	0.00
0.1	0.41
0.2	0.83
0.3	1.45
0.4	2.17
0.5	3.20
0.6	4.65
0.7	7.03
0.8	31.74
0.9	15.82
1.0	0.00

II. Calculated vacuum forces on a 3° gravity foil as calculated using Eq. 6 and the variables listed in Table I

V_w	7.67 m/s (1500 ft/min)
B_1	180.0 mm
B_2	20.0 mm
h_1	Trial A/I = 1.53 mm[b]
h_1	Trial A/II = 1.76 mm[d]
h_1	Trial B/I = 2.14 mm[c]
h_1	Trial B/II = 3.03 mm[e]
h_2	1.0 mm
X	0–1.0 (intervals of 0.1)
μ	0.001 N·s/m^2
P_a	1.0133 × 10^5 N/m^2

[a] Values correspond to conditions reported by Schiher and Getman *(1)*.
[b] Corresponds to step depth (h_1–h_2) of 0.53 mm
[c] Corresponds to step depth (h_1–h_2) of 1.14 mm
[d] Corresponds to step depth (h_1–h_2) of 0.76 mm
[e] Corresponds to step depth (h_1–h_2) of 2.03 mm

III. List of variables required to calculate vacuum forces on Step Foil I using Eq. 4[a]

foil, which is in agreement with the experimental results. Thus the vacuum forces predicted by Eq. 6 agree quite well with the experimental results in Fig. 1.

On the other hand, there is clearly a minor discrepancy between the two profiles at the leading tips (0 ≤ X ≤ 0.5) of the foil, where several wavelike changes in vacuum are apparent in Fig. 1 but not in Fig. 8. This might be explained by the vibration-related upward and downward accelerations caused by the moving fabric *(1)*. Nevertheless, the inability to track these profile variations does not reduce the effectiveness of Eq. 6, since the major contributors to the stock jump on the wire—the main item of concern for papermakers—are the location and force of peak vacuum, both of which were successfully predicted by Eq. 6.

Vacuum force on step foils

Vacuum profiles on different step foils were simulated using Eq. 4. Two step foils (Foils I and II) were simulated based on the geometrical designs depicted in Figs. 2 and 3, respectively. These two figures represent two successive trials (A and B) involving a change in step depth that was large enough to destroy the hydrodynamic pulse. Trial A in Figs. 2 and 3 represents a typical step blade pulse, while Trial B simulates the pulse of a slotted low-vacuum drainage element. The values for the variables used in Eq. 4 are listed in **Tables III** for Step Foils I and II, respectively. Calculated vacuum forces on Step Foils I and II are presented in **Tables IV and V**, respectively.

Table VI compares the calculated values for peak vacuum in Tables V and VI with the measured peak vacuums in Figs. 2 and 3. Peak vacuums of Trials A and B on Foil I were 138 cm H_2O and 40 cm H_2O (Table V), compared with peak values 135 cm H_2O and 25 cm H_2O in Fig. 2. On Foil II, computed peak values were 79 cm H_2O for Trial A and 14.3 cm H_2O for Trial B (Table VI), compared with 76 cm H_2O and 38 cm H_2O in Fig. 3.

These comparisons indicate that for Trial A, the calculated peak values on both foils were almost identical to the measured peak values in Figs. 2 and 3. However, the calculated peak values for Trial B were considerably different from the peak values

X	CALCULATED VACUUM FORCE, cm H_2O Trial A (0.53 mm)	Trial B (1.14 mm)
0.0	0	0
0.1	138	40
0.2	122	35
0.3	107	31
0.4	92	26
0.5	76	22
0.6	61	17
0.7	46	13
0.8	29	9
0.9	15	4
1.0	0	0

IV. Calculated vacuum forces on Step Foil I (step depths of 0.53 and 1.14 mm) as calculated using Eq. 4 and the variables listed in Table III

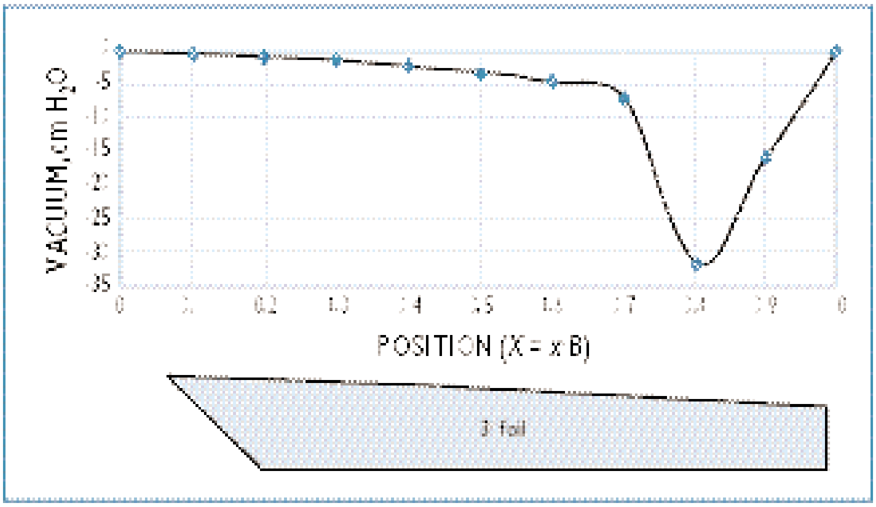

8. Calculated vacuum forces on a gravity foil at machine speed = 8.64 m/s (1700 ft/min)

X	CALCULATED VACUUM FORCE, cm H_2O Trial A (0.76 mm)	Trial B (2.03 mm)
0.0	0	0.0
0.1	79	14.3
0.2	70	12.7
0.3	62	11.1
0.4	53	9.5
0.5	44	7.9
0.6	35	6.3
0.7	26	4.7
0.8	17	3.2
0.9	8	1.6
1.0	0	0.0

V. Calculated vacuum forces on Step Foil II (step depths of 0.76 and 2.03 mm) as calculated using Eq. 6 and the variables listed in Table IV

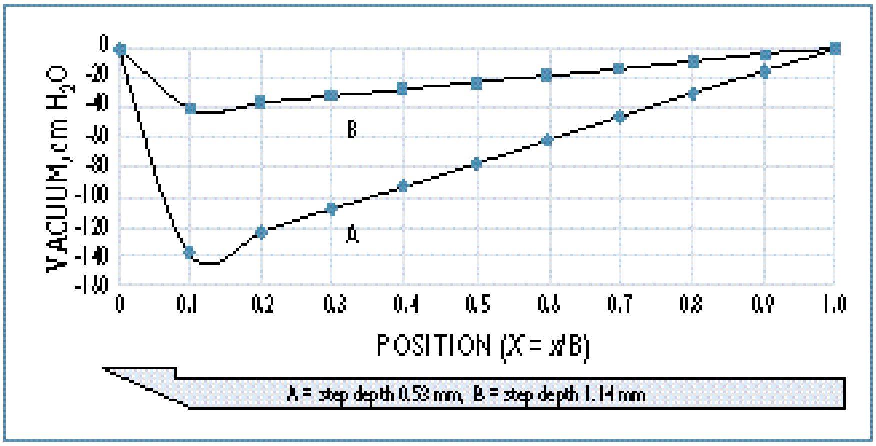

9. Calculated vacuum forces on Step Foil I with step depths of 0.53 mm and 1.14 mm at machine speed = 7.67 m/s (1500 ft/min)

	PEAK VACUUM FORCE, cm H_2O Calcu-lated	Meas-ured	Differ-ence, %
Step Foil I			
Trial A (0.53 mm)	138	135	2.17
Trial B (1.14 mm)	40	25	37.50
Step Foil II			
Trial A (0.76 mm)	79	76	3.79
Trial B (2.03 mm)	14.3	38	–165.73

VI. Comparison of calculated peak vacuums with measured peak vacuums

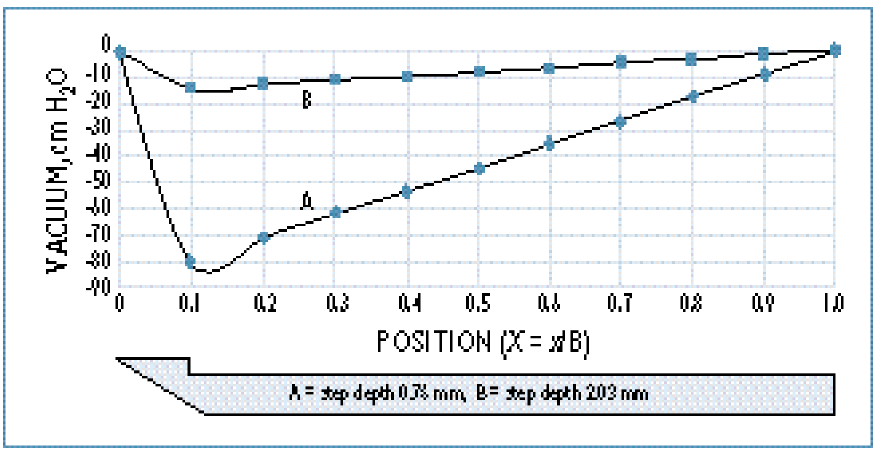

10. Calculated vacuum forces on Step Foil II with step depths of 0.76 mm and 2.03 mm at machine speed = 7.67 m/s (1500 ft/min) that were measured. Clearly, Eq. 4 is not valid in the case of Trial B, but this is not surprising, since there was no hydrodynamic pulse generated during Trial B.

Figures 9 and 10 show the pressure profiles on Step Foils I and II, respectively. In both cases, the peak vacuum occurs near the tips of the foils, closely following the foil steps. This is consistent with Schiher and Getman's observation *(1)* that a sharp vacuum spike is located immediately following the step transition.

CONCLUSIONS

Equations for calculating the vacuum pressures on gravity foils and step foils were developed based on lubrication theory. These equations were then tested by calculating profiles of vacuum pressure across the foils. Comparison of the simulated profiles with experimentally measured vacuum profiles demonstrated the validity of the proposed equations.

The calculated peak pressures for both foil types were within 4% of the measured values, and the simulated vacuum profiles were consistent with measured profiles. For gravity foils, peak vacuum occurs at the tail of the foil. Step foils show the opposite behavior, with peak vacuum occurring near the front tip of the foil, just after the step change. TJ

Zu is an associate professor and Chen is a former graduate student in the Department of Mechanical and Industrial Engineering, University of Toronto, 5 King's College Road, Toronto, ON, Canada M5S 3G8.

Received for review Feb. 18, 1998.
Accepted March 25, 1999.

LITERATURE CITED

1. Schiher, S. C. and Getman, D. L., *TAPPI 1994 Wet-End Operations Short Course Notes*, TAPPI PRESS, Atlanta, Chap. 4-1, pp. 109–126.
2. Gross, W. A., Matsch, L. A., Castelli, V., *et al.*, *Fluid Film Lubrication*, John Wiley & Sons, New York, 1980.
3. Rayleigh, L., *Philos. Mag.* 35: 1(1912).
4. Charnes, A., Osterle, F., and Saibel, F., *ASME Trans.* 77: 33(1995).
5. Maday, C. J., *J. Lubrication Technol.* 90: 240(1968).